SLAC-PUB-16338

Accelerator measurements of magnetically-induced radio emission from particle cascades with applications to cosmic-ray air showers

K. Belov,[1,2] K. Mulrey,[3] A. Romero-Wolf,[2] S. A. Wissel,[1,*] A. Zilles,[4] K. Bechtol,[5] K. Borch,[1] P. Chen,[6] J. Clem,[3] P. W. Gorham,[7] C. Hast,[8] T. Huege,[9] R. Hyneman,[1,10] K. Jobe,[8] K. Kuwatani,[1] J. Lam,[1] T. Liu,[6] J. Nam,[6] C. Naudet,[2] R. Nichol,[11] B. F. Rauch,[12] B. Rotter,[7] D. Saltzberg,[1] H. Schoorlemmer,[7] D. Seckel,[3] B. Strutt,[11] A. G. Vieregg,[5,13] and C. Williams[14]

(T-510 Collaboration)

[1] *Dept. of Physics and Astronomy, Univ. of California, Los Angeles, Los Angeles CA 90095, USA*
[2] *Jet Propulsion Laboratory, Pasadena CA 91109, USA*
[3] *Dept. of Physics, Univ. of Delaware, Newark DE 19716, USA*
[4] *Institut für Experimentelle Kernphysik, Karlsruher Institut für Technologie, 76128 Karlsruhe, Germany*
[5] *Kavli Institute for Cosmological Physics, Univ. of Chicago, Chicago IL 60637, USA*
[6] *Dept. of Physics, Grad. Inst. of Astrophys., National Taiwan University, Taipei Taiwan*
[7] *Dept. of Physics and Astronomy, Univ. of Hawaii, Manoa HI 96822, USA*
[8] *SLAC National Accelerator Laboratory, Menlo Park CA, 94025, USA*
[9] *Institut für Kernphysik, Karlsruher Institut für Technologie, 76021 Karlsruhe, Germany*
[10] *Physics Dept., College of William & Mary, Williamsburg VA 23187, USA*
[11] *Dept. of Physics. Univ. College London, United Kingdom*
[12] *Dept. of Physics, Washington Univ. in St. Louis, St. Louis MO 63130, USA*
[13] *Dept. of Physics, Enrico Fermi Institute, Univ. of Chicago, Chicago IL 60637, USA*
[14] *Dept. of Physics, Stanford Univ., Stanford CA, 94305, USA*

(Dated: July 28, 2015)

An experiment at SLAC provides the first beam test of radio-frequency (RF) radiation from a charged particle cascade in the presence of a magnetic field (up to ∼1 kG), a model system for RF emission from a cosmic-ray air shower. This experiment provides a suite of controlled laboratory measurements to compare to particle-level simulations of RF emission, which are relied upon in ultra-high-energy cosmic-ray air shower detection. We compare simulations to data for intensity, linearity with magnetic field, angular distribution, polarization, and spectral content. In particular, we confirm recent predictions that the magnetically induced emission forms a beam that peaks at the Cherenkov angle and show that the simulations reproduce the data within systematic uncertainties.

PACS numbers: 95.55.Vj, 98.70.Sa, 29.27.-a

PACS numbers: PACS numbers 95.55.Vj, 98.70.Sa

The highest energy cosmic rays arrive at Earth with energies in excess of 10^{20} eV. Despite decades of work meant to uncover their sources, their origin remains elusive. Observations are limited by the low flux at the end of the cosmic-ray spectrum, calling for the development of new techniques with high duty cycles, high precision, and large surface areas. One promising technique makes a measurement of the radio-frequency electric field from a cosmic-ray air shower, which is linear with the energy of the primary particle.

Radio emission arises from the interaction of a cascade of charges moving in the presence of a dielectric, the air, and magnetic field in two main ways. Askaryan radiation forms from a charge excess built up in the shower due to Compton scattering and positron absorption, forming a time-varying current along the shower axis and radio frequency emission [1]. Such emission has been measured in accelerator experiments [2–6]. Geomagnetic emission forms when the Lorentz force acts on charges in the shower, generating a time-varying transverse current. The former is present even with no magnetic field, and the latter is present even without a charge asymmetry. In practice, experiments detect the sum of these two effects.

Several experiments have detected radio emission from cosmic-ray air showers [7–11]. To progress from event detection to measurement of a differential energy flux, one needs to know the intensity and angular distribution of the radio frequency emission and its frequency dependence. To date, predictions of these parameters have relied on simulations and measurements in the field. This work provides a laboratory benchmark for the simulations.

Two formalisms, ZHS [12] and Endpoints [13], are at the heart of recent simulations of radio emission, ZHAireS [14] and CoREAS [15], respectively. They both treat each shower particle track as an independent radiator, summing up the emission from all tracks in the cascade to obtain the signal that would be received by an observer. The ZHS technique has been adapted to the time-domain [16] and calculates the vector potential of each particle track. The Endpoints formalism sums the radiation due to the acceleration between discrete segments of the particles' trajectories [13]. Both formalisms are compared to the accelerator data in this paper.

This material is based upon work supported by the U.S. Department of Energy, Office of Science, Office of Basic Energy Sciences, under Contract No. DE-AC02-76SF00515 and HEP.

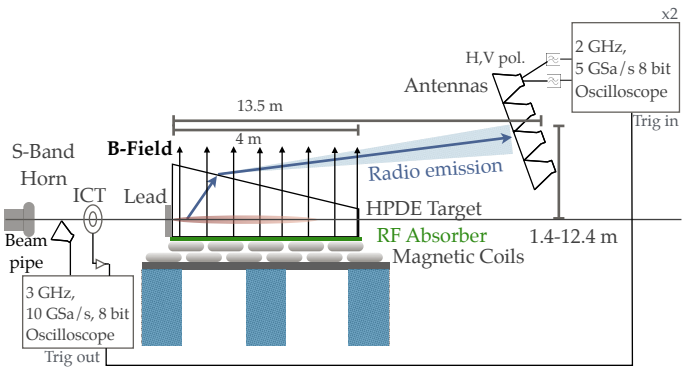

FIG. 1. Schematic of the experiment, not to scale.

FIG. 2. Left: The HPDE target and magnetic field coils. Right: horn antenna array in ESA.

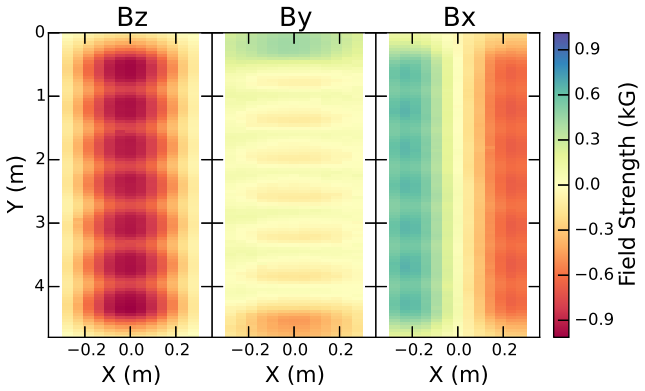

FIG. 3. The measured magnetic field at the beam height along the vertical (z), longitudinal (y), and transverse (x) axes.

The T-510 experiment, shown schematically in Fig. 1, took place at the End Station Test Beam (ESTB) in End Station A (ESA) at SLAC. An electron beam with energy 4.35 or 4.55 GeV passed through two radiation lengths of lead pre-shower and entered a plastic target, generating a particle beam equivalent to the shower maximum of a $\sim 4 \times 10^{18}$ eV primary cosmic ray.

The target, shown in Fig. 2, was formed from 5.08 cm × 10.16 cm × 30.48 cm bricks of high-density polyethylene (HPDE). Being 4 m long, 0.96 m tall, and 0.60 m wide, it contained the majority of the particle shower. The bricks on the top surface were machined to a 9.8 degree angle below horizontal to avoid total internal reflection. The index of refraction of HDPE is 1.53, resulting in a refracted Cherenkov angle of 28° from the horizontal (49° before refraction). Rays emanating from the target at the refracted Cherenkov angle intersected the antenna plane at about 6 m above the position of the beam. The target floor was lined with an RF absorbing blanket. Several pieces of ANW-79 absorber were placed at both sides of the target and at the exit surface of the target.

Fifteen water-cooled coils placed under the target were used to create a vertical magnetic field of up to ±970 G. This was achieved by supplying sets of five coils in series up to 2400 A direct current with reversible polarity. The coils were aligned along the beam axis on a 10.16 cm thick steel plate and were staggered in two rows in order to create a more uniform magnetic field. The magnetic field map at maximum current is shown in Fig. 3, measured at the beam height, 21 cm above the coils. The magnetic field generated by these coils was strong enough to bring the expected intensity from the Askaryan effect and the magnetic effect on the same order of magnitude. There is a 6% scale uncertainty on the magnetic field map, measured using a Hall probe.

Four dual-polarization, quad-ridged horn antennas used in the ANITA experiment [17], sensitive to the 200-1200 MHz band, recorded the electric fields generated in the particle shower. An overhead crane allowed for the movement of the antenna array to sample the electric field at many positions. The antenna array was placed at the far wall of ESA, 13.5 m from the entrance of the beam to the target. It was tilted at 19.6° to better align the expected radiation with the boresight of the antennas. The antenna array covered vertical distances between 1.5 m and 12.5 m, corresponding to angles between 40° and 55° from shower maximum.

Signals from each antenna ran through 15.24 m of LMR240 coaxial cable and a low-pass filter with a 3 dB point of 1250 MHz to avoid aliasing during data acquisition. Time-series voltages from the horns were collected on 2.0 GHz, 5 GSa/s oscilloscopes. A global trigger was provided by the broadband transition radiation produced by the beam exiting the beam pipe, collected in an S-band horn antenna. Events were recorded at 1 Hz.

The beam charge was measured using an integrating charge transformer situated between the beam pipe and the target. The mean bunch charge was 131 pC, with a

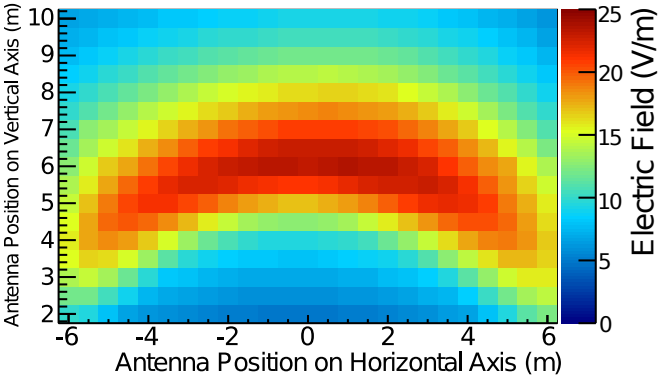

FIG. 4. Simulated (Endpoints) electric field in the detection plane with full magnetic field, 131 pC, and 4.35 GeV.

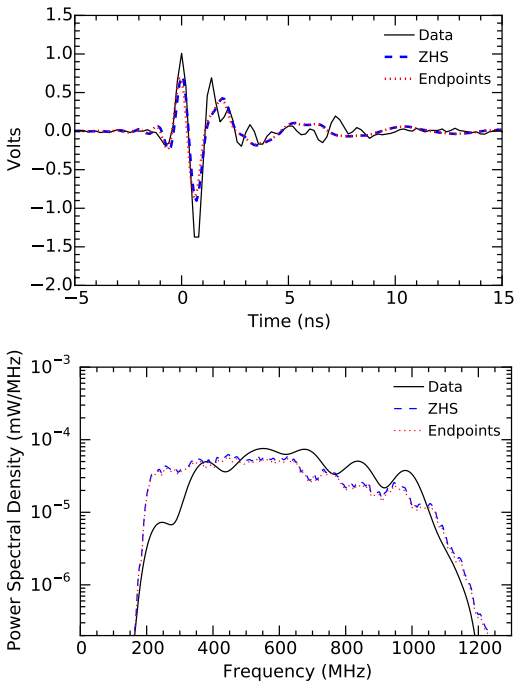

FIG. 5. Top: simulated and measured voltages 6.52 m above the beam in the horizontal polarization channel at full magnetic field. Bottom: corresponding power spectral densities.

shot-to-shot standard deviation of 3 pC. Measurements of the bunch charge at several positions indicate a 2% systematic uncertainty.

Particle showers were simulated with GEANT4. The radio emission was then simulated following the ZHS and Endpoints formalisms. For each track, we included refraction, Fresnel coefficients, and demagnification effects [18] at the surface of the target in the calculations. The Endpoints simulation, shown in Fig. 4, demonstrates that expected radiation forms a conical beam when projected onto a two-dimensional plane 13.5 m from the entrance to the target, peaking at about 6.5 m above the beam. Refraction at the target surface makes the cone elliptical rather than circular. The ring is cut off on both sides due to the finite target. The ∼20% net negative charge excess of the shower combined with interference effects generates an asymmetry in the observed and simulated cones. Effects due to transition radiation are were estimated and found to be two orders of magnitude below the Askaryan radiation.

Because the magnetic field is vertical at the shower, the signal of interest is primarily horizontally polarized. We also expect, and see, a significant signal in the vertical polarization due to the Askaryan effect, which does not depend on magnetic field. In our antennas, the vertical signal will leak into the horizontally polarized channel at about the 25% level in amplitude (about −12 dB in power). We eliminate this leakage by construction using the difference between field-up, $V_{B_+}(t)$, and field-down, $V_{B_-}(t)$, data, namely $V(t) = \frac{1}{2}(V_{B_+}(t) - V_{B-}(t))$. Each waveform is also scaled by the shot beam charge to 131 pC. This is measured by the amplitude of the transition radiation from the beam exiting the vacuum window, as recorded by the S-band horn pointed at the exit of the beam pipe. The resulting waveform from the horizontal polarization at maximum magnetic field strength is shown in the top plot of Fig. 5. The lower figure shows the power spectral density normalized by the sampling interval 200 ps/point for the data and 100 ps/point for the simulations [19].

For comparison, the simulated electric fields were convolved with the measured antenna effective heights [17] and response due to the cables and filters used in the system. The convolution was performed in the frequency domain following standard techniques [20]. The predicted values in Fig. 5 from the two different formalisms agree to within 3% in peak amplitude and 7% in integrated power. The dominant features in the time-domain waveform arise from antenna response and filters, which the two simulations have in common. The shape of the simulated waveforms reproduces the data well, giving us confidence in the experimental modeling. The absolute scale is discussed below.

Reflections from the bottom of the target interfered with the main pulse, which is apparent in the modulation of the power spectral density versus frequency. From the geometry and assuming that the absorber has a higher index of refraction than the HPDE, we infer that one reflection arrived at a given antenna position ∼1 ns after the main pulse with inverted polarity, and largely constructively interfered with it. A second reflection bounced off the top of the target and again off the bottom surface, arriving ∼4-6 ns after the first pulse. Adding in a reflection equivalent in amplitude to the the initial pulse at the time expected from geometry varies the simulated peak time-domain amplitude by a factor of 1.38 for horizontal polarization and 1.43 for vertical polarization. This leads to an uncertainty of 38% and 43% in the two polariza-

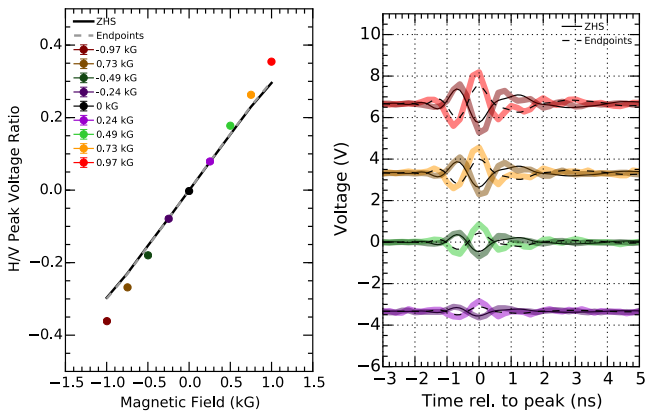

FIG. 6. Left: horizontally polarized signal normalized by vertical showing the expected linear behavior vs. magnetic field. Right: the oscilloscope traces (some offset for clarity) show the polarity flip. Models are shown for opposite polarities.

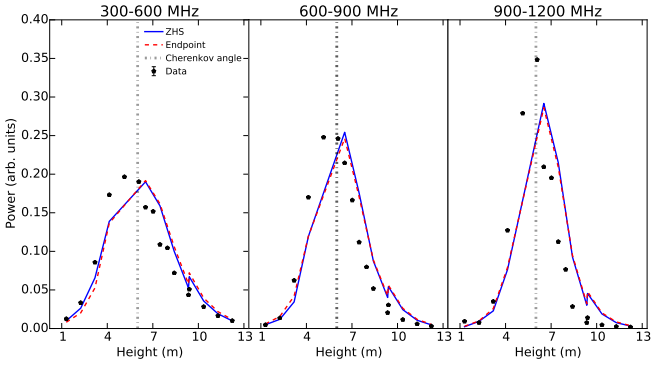

FIG. 7. Beam patterns for three frequency bands in the horizontal polarization at 970 G.

tions on the models due to the reflection, averaged over the band 300-1200 MHz. We exclude the 200-300 MHz band in the data and simulation comparisons due to uncertainty in the antenna response at low frequencies. For the horizontal polarization, the time-domain peaks of the data and the Endpoints simulation differ by 36% and from the ZHS simulation by 34%, commensurate with the systematic uncertainty.

Fig. 6 shows several predicted behaviors using the time-domain peak amplitudes. The strength of the horizontally polarized emission is linearly dependent on the magnetic field. The polarity of this induced voltage changes sign when the direction of the magnetic field flips direction, indicating that the transverse current flows in the opposite direction. The vertically polarized emission is observed to be constant with respect to magnetic field strength.

Several aspects of the radio emission in cosmic-ray air showers contribute to the formation of a conical beam pattern centered around the Cherenkov angle [21, 22]. In this experiment, different angles were probed at different vertical positions. The power profile, which traverses the expected peak of the cone, is shown in Fig. 7 for three different frequency bands. Each profile is normalized by its total power. Because coherence is a function of wavelength, the cone grows narrower with increasing frequency.

We present the first laboratory measurements of radio-frequency radiation from particle showers under the influence of a magnetic field. The emission grows linearly with magnetic field strength and forms a conical beam centered around the Cherenkov angle. Both the ZHS and Endpoints formalisms agree and reproduce the data to within the systematic uncertainty, with the largest uncertainty arising from reflections in our target. This work establishes the first laboratory benchmark for the absolute energy scale of radio emission produced by cosmic rays. The cosmic ray energy spectrum is essentially featureless, and interpretation of astrophysical observations relies critically on knowing the energy of the events. This confirmation will directly impact observations by current experiments such as ANITA [17] , LOFAR [9], CODALEMA [8], and AERA [10]. It also strengthens the case for proposed experiments based in the radio technique such as the EVA balloon mission [23], the SWORD satellite mission [24], the mountain-top observatory TAROGE, and others.

The authors thank SLAC National Accelerator Laboratory for providing facilities and support and especially Janice Nelson and Carl Hudspeth for their support and dedication that made T-510 possible. We thank D. Z. Besson for helpful discussions. This material is based upon work supported by the Department of Energy under Award Numbers DE-AC02-76SF00515, DE-SC0009937, and others. Work supported in part by grants from the National Aeronautics and Space Administration and the Taiwan Ministry of Science and Technology under project number MOST103-2119-M-002-002, among others. Part of this research was funded through the JPL Internal Research and Technology Development program. This work was supported in part by the Kavli Institute for Cosmological Physics at the University of Chicago through grant NSF PHY-1125897 and an endowment from the Kavli Foundation and its founder Fred Kavli. We are grateful to the ANITA collaboration for use of antennas and other equipment.

* Corresponding author: swissel@physics.ucla.edu

[1] G. A. Askaryan, JETP **14**, 441 (1962).
[2] D. Saltzberg *et al.*, Phys. Rev. Lett. **86**, 2802 (2001).
[3] P. W. Gorham *et al.*, Phys. Rev. E **62**, 8590 (2000).
[4] P. W. Gorham *et al.*, Phys. Rev. D **72**, 023002 (2005).
[5] P. W. Gorham *et al.*, Phys. Rev. Lett. **99**, 171101 (2007).
[6] P. Miočinović *et al.*, Phys. Rev. D **74**, 043002 (2006).

[7] H. Falcke *et al.*, Nature **435**, 313 (2005).
[8] D. Ardouin *et al.*, Astropart. Phys. **26**, 341 (2006).
[9] P. Schellart *et al.*, A&A **560**, A98 (2013).
[10] A. Aab *et al.*, Phys. Rev. D **89**, 052002 (2014).
[11] S. Hoover *et al.*, Phys. Rev. Lett. **105** (2010).
[12] E. Zas, F. Halzen, and T. Stanev, Phys. Rev. D **45**, 362 (1992).
[13] C. W. James, H. Falcke, T. Huege, and M. Ludwig, Phys. Rev. E **84**, 056602 (2011).
[14] J. Alvarez-Muñiz, W. R. Carvalho, and E. Zas, Astropart. Phys. **35**, 325 (2012).
[15] T. Huege, M. Ludwig, and C. W. James, AIP Conf. Proc. **1535**, 128 (2013).
[16] J. Alvarez-Muñiz, A. Romero-Wolf, and E. Zas, Phys. Rev. D **81**, 123009 (2010).
[17] P. W. Gorham *et al.*, Astropart. Phys. **32**, 10 (2009).
[18] N. G. Lehtinen *et al.*, Phys. Rev. D **69**, 013008 (2004).
[19] W. H. Press *et al.*, *Numerical recipes: The Art of Scientific Computing* (Cambridge University Press, 2007).
[20] Krauss, J. D., *Antennas* (MacGraw-Hill, 1988).
[21] K. Belov *et al.*, AIP Conf. Proc. **1535**, 209 (2013).
[22] K. D. de Vries *et al.*, Phys. Rev. Lett. **107**, 061101 (2011).
[23] P. W. Gorham *et al.*, Astropart. Phys. **35**, 242 (2011).
[24] A. Romero-Wolf *et al.*, arXiv:1302.1263 [astro-ph.IM] (2013).